LWT - Food Science and Technology 131 (2020) 109761

Contents lists available at ScienceDirect

LWT - Food Science and Technology

journal homepage: www.elsevier.com/locate/lwt

Use of an NIR MEMS spectrophotometer and visible/NIR hyperspectral imaging systems to predict quality parameters of treated ground peppercorns

Carlos A. Esquerre[a,*], Eva M. Achata[a], Marco García-Vaquero[b], Zhihang Zhang[c], Brijesh K. Tiwari[c], Colm P. O'Donnell[a]

[a] School of Biosystems and Food Engineering, College of Engineering and Architecture, University College Dublin, Dublin, D04V1W8, Ireland
[b] School of Agriculture and Food Science, College of Health and Agricultural Sciences, University College Dublin, Dublin, D04V1W8, Ireland
[c] Department of Food Chemistry and Technology, Teagasc Food Research Centre, Ashtown, Dublin, D15KN3K, Ireland

ARTICLE INFO

Keywords:
NIR MEMS
Hyperspectral imaging
Antioxidant capacity
Total phenolic content
Peppercorn

ABSTRACT

The aim of this study was to investigate the potential of a micro-electromechanical NIR spectrophotometer (NIR-MEMS) and visible (Vis)/NIR hyperspectral imaging (HSI) systems to predict the moisture content, antioxidant capacity (DPPH, FRAP) and total phenolic content (TPC) of treated ground peppercorns. Partial least squares (PLS) models were developed using spectra from peppercorns treated with hot-air, microwave and cold plasma. The spectra were acquired using three spectroscopy systems: NIR-MEMS (1350–1650 nm), Vis-NIR HSI (450–950 nm) and NIR HSI (957–1664 nm). Very good predictions of TPC (RPD > 3.6) were achieved using NIR-MEMS. The performance of models developed using Vis-NIR HSI and NIR HSI were good or very good for DPPH (RPD > 3.0), FRAP (RPD > 2.9) and TPC (RPD > 3.8). This study demonstrated the potential of NIR-MEMS and Vis-NIR/NIR HSI to predict the moisture content, antioxidant capacity and total phenolic content of peppercorns. The spectroscopy technologies investigated are suitable for use as in-line PAT tools to facilitate improved process control and understanding during peppercorn processing.

1. Introduction

Pepper (*Piper nigrum* L.) is a widely used spice (Meghwal & Goswami, 2013; Shityakov et al., 2019). Black, green and white peppercorns are obtained from the same plant species but differ in the manner of preparation for the market, resulting in different flavours and degrees of spiciness (Nikolić et al., 2015). Black peppercorns are prepared by briefly cooking and drying the unripe corns, white peppercorns consist of the dried ripe corns with the outer pericarp removed, while green peppercorns are harvested unripe and then dried (Friedman et al., 2008; Meghwal & Goswami, 2013). The *Piper nigrum* L. plant is rich in essential oil (2–3%) and is a source of numerous biologically active constituents such as monoterpenes, sesquiterpenes, and other volatile compounds (Nikolić et al., 2015). Piperine is the major pungent alkaloid present in the corns of *Piper nigrum* L. and is associated with immunomodulatory, anti-oxidant, anti-asthmatic, anti-carcinogenic, anti-inflammatory, anti-ulcer, anti-amoebic (Meghwal & Goswami, 2013) and diuretic properties (Shityakov et al., 2019). Pink peppercorns (*Schinus terebinthifolius*) are used as condiments and have a high demand in the spice market. Extracts rich in phenolic substances from the residues of the pink pepper tree processing industry exhibited significant activity against multidrug-resistant bacteria (Gomes et al., 2020).

Preservation of peppercorns may be achieved by application of several process treatments which reduce the moisture content and/or improve microbial quality. Hot air drying is the most widely employed processing treatment for peppercorns. Recent studies have proposed the use of microwave assisted drying and cold plasma (Charoux et al., 2020) for peppercorn processing. Peppercorns treated with microwaves had improved retention of the main aroma compounds (Plessi, Bertelli, & Miglietta, 2002). The use of microwaves combined with hot air drying increases the efficiency of the drying process, improves moisture uniformity, shortens the drying time while reducing thermal effects on bioactives (Schiffmann, 2014). Cold plasma is a non-thermal technology that has been used as an alternative for microbial inactivation in solid and liquid foods (Charoux et al., 2020; Misra et al., 2014). Montenegro, Ruan, Ma, and Chen (2002) reported that cold plasma discharges applied directly to the food product proved effective in

* Corresponding author.
E-mail address: carlos.esquerre@ucd.ie (C.A. Esquerre).

https://doi.org/10.1016/j.lwt.2020.109761
Received 11 March 2020; Received in revised form 15 May 2020; Accepted 14 June 2020
Available online 15 June 2020

reducing the number of *Escherichia coli* O157:H7 cells in apple juice, by up to 7 log units.

Quality and process control measurements in the food industry are frequently carried out off-line in laboratories rather than on-line. The resultant delay incurred between sampling and measurement limits optimisation and control of production processes. Adoption of in-line process analytical technology (PAT) tools leads to an improved understanding of both the process and product variability (O'Donnell, Fagan, & Cullen, 2014). This enhanced understanding enables efficient process control strategies and real-time process feedback, as well as continuous knowledge building of the process itself (O'Donnell et al., 2014). Potential benefits of PAT adoption are considerable and include higher quality products, improved product consistency and reduced manufacturing costs (Pu, O'Donnell, Tobin, & O'Shea, 2020). Visible (Vis)/NIR spectroscopy is one of the most promising sensing approaches for in-line control of peppercorns preservation processing (Lapcharoensuk et al., 2019; Orrillo et al., 2019; Wilde, Haughey, Galvin-King, & Elliott, 2019). The advantages of spectroscopic methods for bioprocess monitoring are manifold and include real-time capability, non-destructive nature, ease of maintenance and the possibility for simultaneous determination of multiple target analytes (Zimmerleiter et al., 2019). NIR combined with multivariate data analysis has been previously used for rapid determination of piperine and other pepper oil components in black and white ground pepper (Schulz, Baranska, Quilitzsch, Schütze, & Lösing, 2005), and to detect adulteration of ground black pepper (Wilde et al., 2019). Challenges to the adoption of Vis-NIR spectroscopy for in-line process control applications include PAT tool robustness in a plant environment, limited field of view and the development of the chemometric models required.

Advances in microelectromechanical systems (MEMS), semiconductors, computing capabilities, and chemometrics have allowed the miniaturisation of systems for field and inline applications (Rodriguez-Saona & Aykas, 2019). MEMS transducers are fabricated using solid-state micromachining techniques commonly used by the semiconductor industry in the production of integrated circuits (Mendelson, 2012). Miniature spectrophotometers which use MEMS technology are compact, robust and relatively low cost devices (Zimmerleiter et al., 2019). MEMS-based Fabry-Perot interferometers have been employed in miniaturised NIR spectrophotometers (Yan & Siesler, 2018). The use of common optical paths in Fabry-Perot interferometers (FPI) make them less sensitive to environmental disturbances than Michelson interferometers which use different optical paths (Wang, Shyu, & Chang, 2010). MEMS based FPI usually consist of a vertically integrated structure composed of two mirrors separated by an air gap, wavelength tuning is achieved by applying a voltage between the two mirrors resulting in an electrostatic force which pulls the mirrors closer. However the main disadvantage associated with two-mirror FPI is limited spectral range (Parashar, Shah, Packirisamy, & Sivakumar, 2007).

Hyperspectral imaging also known as chemical or spectroscopic imaging, is a PAT tool for food quality and safety control that integrates conventional imaging and spectroscopy to obtain both spatial and spectral information from a sample (Gowen, O'Donnell, Cullen, Downey, & Frias, 2007). Use of hyperspectral imaging systems facilitate improved inspection of raw material, in-process and final product. Hyperspectral images or hypercubes consist of several congruent images representing intensities at different spectral bands and spatial positions. These hypercubes are three-dimensional blocks of data, comprising one spectral (λ) and two spatial dimensions (X, Y). Each pixel in a hyperspectral image contains the spectrum of that specific position, representing the light-absorbing and/or scattering properties of the spatial region represented, which can be used to characterise the composition of that particular pixel (Gowen et al., 2007). NIR-HSI has been evaluated for prediction of black pepper adulteration with papaya seeds (Orrillo et al., 2019) and to identify samples treated with selected preservation technologies (Achata, Inguglia, Esquerre, Tiwari, & O'Donnell, 2019).

Principal component analysis (PCA) is frequently employed as an exploratory tool in chemometric analysis of Vis-NIR spectral data. PCA transforms a spectral dataset with highly correlated spectral bands into a smaller set of uncorrelated components. This reduces the original dataset, filtering noise and redundancies based on the variance–covariance structure of the original data, to reveal hidden and simplified structure/patterns (Mujica, Rodellar, Fernández, & Güemes, 2010). Partial least squares (PLS) is the most commonly used regression method to predict composition or quality parameters using Vis-NIR spectroscopy data. Spectral pre-treatments may be employed to correct for the effects of light scattering and differences in the effective path length on Vis-NIR spectra and improve the performance of PLS models (Esquerre, Gowen, Burger, Downey, & O'Donnell, 2012). Variable selection methods have also improved the performance of Vis-NIR PLS models and reduced the processing times required by selecting the most informative wavelengths (Achata et al., 2019).

The aim of this study was to investigate the use of an NIR MEMS spectrophotometer and Vis-NIR/NIR hyperspectral imaging systems to predict the moisture content, antioxidant capacity and total phenolic content of treated ground peppercorns.

2. Materials and methods

2.1. Peppercorn samples

Black, white and green (*Piper nigrum*) and pink peppercorns (*Schinus terebinthifolius*) were used in this study. Black peppercorns produced in India were purchased from East End Foods PLC (West Bromwich, UK). White, green and pink peppercorns were purchased from Greenfields (London, UK). All the samples were ground using a blender mill (Cookworks, China) and sieved to 1 mm particle size using a sieve-shaker (VWR International LLC, Ireland). Ground peppercorn samples of each type (i.e. black, white, green and pink peppers) were grouped into 41 subsamples of 5 g each for treatment as described in section 2.2 (n = 4 peppercorn types × 41 subsamples = 164).

2.2. Process treatments of ground peppercorns

The following treatments were applied to the ground peppercorns samples: (1) hot air drying (Drying chamber E28, Binder, Germany) at selected temperatures (40, 60, 80 or 100 °C) and treatment times (5, 10, 15 and 20 min) (n = 4 temperatures × 4 times × 4 peppercorn types = 64); (2) microwave oven-drying (NN-CF778S, Panasonic, UK) at selected power levels (250, 400, 600 or 1000 W) and treatment times (1, 2, 3 and 5 min) (n = 4 power levels × 4 times × 4 peppercorn types = 64); and (3) cold plasma treatment (Leap100, PlasmaLeap Technologies, Ireland) at selected voltages (150 and 300 V) and treatment times (5, 10, 15 and 20 min) (n = 2 voltage × 4 time × 4 peppercorn type = 32). Treated (n = 160) and control samples (n = 4) were placed in a desiccator for 20 min, packed and stored in dark conditions prior to analyses. Treated and control samples' spectra were acquired as described in section 2.4. Each sample was split for moisture analysis (1 g) and for antioxidant capacity and total phenolic analyses (2 g, Section 2.3). Moisture content was determined by oven-drying the samples at 105 °C for 16 h.

2.3. Antioxidant capacity and total phenolic content analyses

All ground peppercorn samples (n = 164) were further processed for antioxidant capacity and total phenolic content analyses. Briefly, ground peppercorn samples were mixed thoroughly with an 80% methanolic solution (1:10, w/v) and placed in an orbital shaker (Heildolph instruments, Schwabach, Germany) at 170 rpm at room temperature overnight. The extracts were filtrated, evaporated, freeze-dried and stored at −20 °C before further analyses. All chemical determinations were performed in duplicate with 3 measurements for each replication (n = 6).

2.3.1. DPPH activity

The 1,1-Diphenyl-2-Picryl-Hydrazyl (DPPH) activity was measured following the method proposed by Nicklisch and Waite (2014), with the modifications described by Garcia-Vaquero, O'Doherty, Tiwari, Sweeney, and Rajauria (2019). Pepper extracts and ascorbic acid were assayed at 1 mg per mL of working solution (0.1 M citrate phosphate buffer with 0.3% of Triton X-100). The reaction was performed in a Greiner 96 flat-bottomed microplate by adding 10 μL of a 2 mM DPPH solution in methanol to each well. The percentage of DPPH inhibition per mg of extract was calculated by subtracting the absorbance readings of each well at 515 nm prior to DPPH solution addition and at 30 min after DPPH solution addition.

2.3.2. FRAP activity

The ferric reducing antioxidant power (FRAP) was determined using the method described by Benzie and Strain (1996) with the modifications as described by Garcia-Vaquero et al. (2019). Briefly, pepper extracts were assayed against trolox standards in a working solution containing 10:1:1:1.4 of acetate buffer (300 mM, pH 3.6), ferric chloride (20 mM in Milli-Q water), 2,4,6-Tripyridyl-s-Triazine (TPTZ) (10 mM in 40 mM HCl) and Milli-Q water. The reaction was performed in 96 well plates (Greiner Bio-one, Germany) and incubated at 37 °C for 30 min. The absorbance of the reaction was measured at 593 nm using an UV–Vis spectrophotometer (Epoch™ 2, Biotek, VT, USA). FRAP values were expressed as mM trolox equivalents (TE) per 100 g sample.

2.3.3. Total phenolic content

The total phenolic content (TPC) of the pepper extracts was determined according to the method described by Ganesan, Kumar, and Bhaskar (2008) with slight modifications. Briefly, samples at appropriate dilutions were assayed together with gallic acid as standard. 2 mL of a Na_2CO_3 solution (2%, w/v) were added to 100 μL of the tested extracts. The solutions were mixed with 100 μL of Folin-Ciocalteu phenol reagent (0.5 M) and allowed to stand for 30 min in dark conditions. The absorbance of the reaction was measured at 720 nm using an UV–Vis spectrophotometer (Epoch™ 2, Biotek, VT, USA). The total phenolic content (TPC) of the samples was expressed as mg gallic acid equivalents (GAE)/100 g sample.

2.4. Spectra acquisition

2.4.1. NIR MEMS spectrophotometer

Ground peppercorn spectra were acquired using an NIR-MEMS spectrophotometer (NIROne, Spectral Engines Oy, Finland) in the range of 1350–1650 nm at 2 nm intervals. The miniaturised NIR-MEMS spectrophotometer consisted of a single element InGaAs detector, a Fabry-Perot interferometer, two tungsten vacuum lamps and an USB interface to a laptop. Black reference (*Ib*) was recorded after turning off the lamp, while the white reference (*Iw*) was recorded using a Thorlab white reference target SM05CP2C (Thorlabs GmbH, Germany) and setting the lamp power to 100%. Samples spectra (*Is*) were acquired and reflectance calculated according to $R = (Is - Ib)/(Iw - Ib)$.

2.4.2. Vis-NIR hyperspectral imaging systems

Hyperspectral images of ground peppercorn were obtained using two line scanning hyperspectral imaging systems (DV Optics, Padova, Italy), one in the visible-near infrared (Vis-NIR) range of 400–1000 nm with a spectral resolution of 5 nm and the other in the near infrared (NIR) range of 880–1720 nm with a spectral resolution of 7 nm. The Vis-NIR HSI system consisted of a CCD camera (580 × 580 pixels; Basler, Ahrensburg, Germany), a spectrograph (Spectral Imaging Ltd., Oulu, Finland), cylindrical light diffuser and moving base. The NIR-HSI system consisted of an InGaAs camera (320 × 240 pixels; Sensors Unlimited, Inc., Princeton, NJ, USA), a spectrograph (Spectral Imaging Ltd., Oulu, Finland), five halogen lamps (3 × 50 W and 2 × 20 W), a cylindrical light diffuser, moving base and a computer (Hernández-Hierro et al., 2014). The speed of the moving base was set at 3 mm/s (spatial resolution 0.28 × 0.28 mm pixel size) and 20 mm/s (spatial resolution 0.3 × 0.3 mm pixel size) for the Vis-NIR and NIR systems respectively. After scanning 50 lines of black reference and 50 lines of a white tile (reflectance > 93%) with a known reflectance (*Rw*) the signal from the sample was converted and stored as reflectance $R = Rw\ (Is - Ib)/(Iw - Ib)$ (Achata, Esquerre, O'Donnell, & Gowen, 2015).

Hyperspectral imaging of all samples was carried out at room temperature (~20 °C). Acquired 3-D data hypercubes were saved in ENVI formatted files and imported into MATLAB (The MathWorks Inc., Natick, MA, USA) for further spectral data pre-processing and data analysis, using in-house developed functions and scripts. The spectra obtained from both HSI systems were trimmed to spectral ranges of 450–960 nm and 957–1664 nm to remove noise at both ends of the spectra. Hypercubes were unfolded by rearranging the three-dimensional hypercubes (X, Y, λ) into a two-dimensional matrix (X × Y) to facilitate algorithm development. Regions of interest (ROI) were carefully selected from each sample to avoid edge effects detected following analysis of PCA scores maps. Mean spectra of each sample were calculated from the selected ROI and used for model development.

2.5. Principal component analysis

PCA of standard normal variate (SNV) pretreated spectral datasets was carried out to investigate the relationships between the peppercorn samples and spectra acquired using the 3 spectroscopy systems, and also to identify potential outliers using the T^2 statistic. A sample was considered as an outlier if the T^2 value was $> T^2_{crit} = A \times F_{(0.05,A,n-A)} \times (n\text{-}1)/(n\text{-}A)$, where A is the number of significant components, n is the number of spectra in the dataset and $F_{(0.05,A,n-A)}$ is the F statistic (with $\alpha = 0.05$, A and $n - A$ degrees of freedom).

2.6. Development of prediction models

PLS regression models to predict moisture, antioxidant capacity and total phenolic content of samples were developed using spectral data, spectral pre-treatments and the ensemble Monte Carlo variable selection (EMCVS) method. SNV, median scaled (MS), Savitzky-Golay 7 points second order polynomial first derivative (FD), Savitzky-Golay 7 points second order polynomial second derivative (SD), Savitzky-Golay 11 points fourth order polynomial third derivative (TD), linear detrending second-order polynomial (LD), asymmetric least squares (AsLs) and all combinations of any two spectral pre-treatments were tested. The EMCVS method was employed to select the bands that produce the most stable regression coefficients (Esquerre, Gowen, O'Gorman, Downey, & O'Donnell, 2017). The spectral datasets were split randomly into calibration and validation datasets. The number of latent variables in the PLS model were selected using the root mean square of 10-fold cross validation and a jaggedness of the regression vector to avoid overfitting (Gowen, Downey, Esquerre, & O'Donnell, 2011).

The performance of the regression models was assessed using the root mean square error (RMSE), the coefficient of determination (R^2), the ratio of standard deviation of the reference data and the RMSE (RPD) for cross-validation and validation sets. The best model was selected based on the number of latent variables, selected wavebands and the geometric mean of the RPD values from calibration (n = 123) and validation (n = 41) sets. The performance of the prediction models based on RPD values for complex matrices can be classified as excellent (RPD > 4.1), very good (RPD 3.5–4.0), good (RPD 3.0–3.4), fair (RPD 2.5–2.9) and poor (RPD 2.0–2.4) (Williams, 2014). It is not recommended to use a prediction model when the RPD values are in the range 0.0–1.9.

3. Results and discussion

3.1. Ground peppercorn moisture, antioxidant capacity and TPC

The moisture, antioxidant capacity (DPPH and FRAP) and TPC of control black, white, green and pink peppercorn samples are summarised in Table 1. Pink peppercorn samples had higher TPC and antioxidant activities than the other peppercorn types. White peppercorn samples had the lowest levels of all analysed parameters. The high TPC values in pink peppercorns (*Schinus terebinthifolius*) may be due to interspecies variation with respect to *Piper nigrum* L. (black, white and green peppercorns). Similar variations were reported by Shan, Cai, Sun, and Corke (2005) with TPC values ranging from 0.30 to 0.78 g GAE per 100 g DW in black, white and green peppercorns. Differences in TPC values between black and white peppercorns were also investigated by Agbor, Vinson, Oben, and Ngogang (2006), with a higher concentration of TPC in black compared to white peppercorns reported.

3.2. Ground peppercorn spectra

Fig. 1 shows the mean spectra of the control samples acquired using the three spectroscopy systems i.e. NIR-MEMS, Vis-NIR HSI and NIR HSI. The NIR-MEMS spectra of the control samples were similar. A broad absorption band may be observed around 1468 nm (Fig. 1a) which can be attributed to the first overtone of the H–OH bond (Rodriguez-Saona, Ayvaz, & Wehling, 2017; Segtnan, Sasic, Isaksson, & Ozaki, 2001). Large variations may be observed between the Vis-NIR HSI spectra of the control samples (Fig. 1b). The main difference between the spectra is the sharp absorption band around 665 nm in the green peppercorn spectra which is related to chlorophyll content (Seifert & Zude-Sasse, 2016). The NIR-HSI spectra of the control samples have similar profiles. In addition to a broad band at 1468 nm, an absorption band around 1202 nm may observed which can be attributed to the 2nd overtone of C–H bond stretching (Fig. 1c). Shoulders are also observed around 1272 nm (water-protein interaction), 1363 nm and 1580 nm in the NIR-HSI spectra.

3.3. Principal component analysis

PCA of SNV pretreated spectra (n = 164) of the ground peppercorn samples identified three samples as outliers using the T^2 statistic. The first three PCs of the remaining ground peppercorn SNV treated spectra (n = 161) from the NIR-MEMS, Vis-NIR HSI and NIR HSI systems are shown in Fig. 2. Good separation of the four types of peppercorn was observed in the PC score plots for the 3 spectroscopy systems (Fig. 2). Ninety two % of the variance in the NIR-MEMS data was explained by the first two principal components PC1 (73%) and PC2 (19%). PC1 loadings were largely influenced by the absorption bands attributed to weakly (1410 nm) and strongly (1456 nm) H-bonded water (Segtnan et al., 2001). Whereas 98% of variance in the Vis-NIR HSI data were explained by the first two principal components PC1 (54%) and PC2 (44%). PC1 loadings were mainly influenced by absorption bands at 650 nm which may be attributed to chlorophyll (Seifert & Zude-Sasse, 2016). In the NIR-HSI spectra PC1 explained 93.2% of the variance with PC1 loadings mainly influenced by the absorption bands at 1216, 1342, 1412 and 1643 nm which may be attributed to the 2nd overtone of C–H bond stretching, the combination of $–CH_2$, first overtone of –OH stretching in water and first overtone of aromatic –CH respectively (Kumagai et al., 2003; Rodriguez-Saona et al., 2017; Šašić & Ozaki, 2000).

Table 1
Moisture, DPPH, FRAP and TPC of control ground peppercorn samples.

Peppercorn type	Moisture (g/100 g sample)[a]	DPPH (%)[a]	FRAP (mM TE/100 g sample)[a]	TPC (mg GAE/ 100 g sample)[a]
Black	10.9 ± 0.2	83.0 ± 2.1	1005 ± 87	633 ± 35
White	11.1 ± 0.2	57.0 ± 3.9	279 ± 4	156 ± 6
Green	8.5 ± 0.1	90.8 ± 0.8	3089 ± 512	832 ± 52
Pink	13.2 ± 0.2	98.9 ± 1.1	8336 ± 164	2761 ± 193

[a] Values represents mean ± standard error (n = 2).

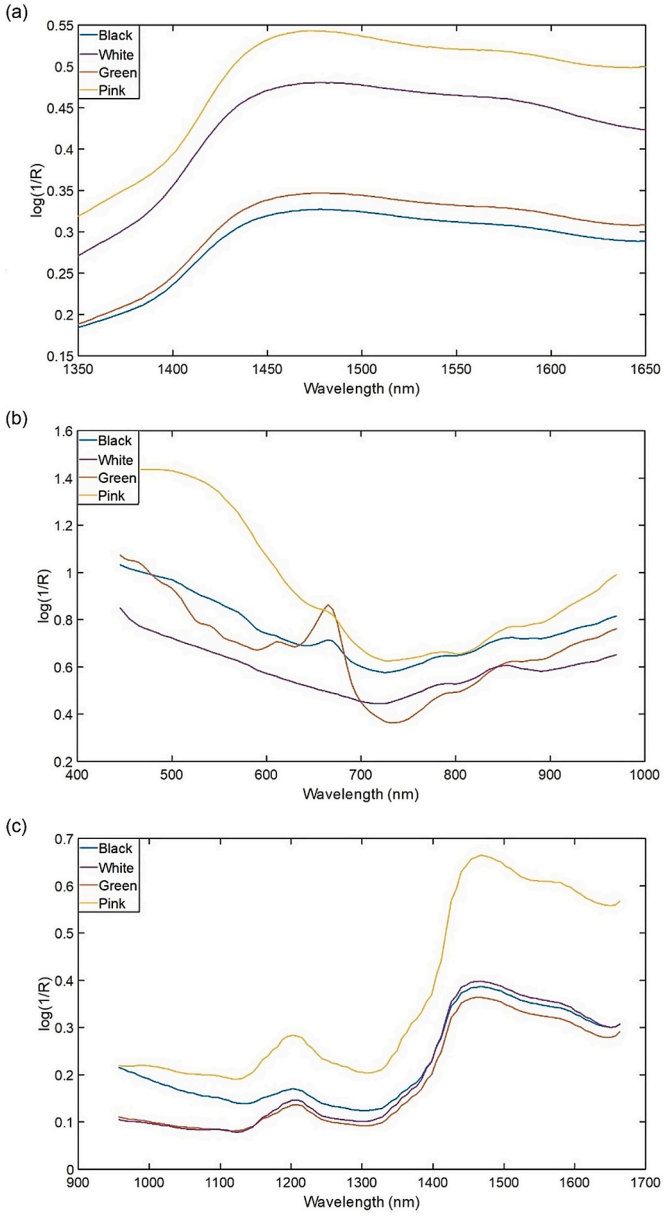

Fig. 1. Mean spectra of control samples of black, white, green and pink ground peppercorn samples acquired using (a) NIR-MEMS, (b) Vis-NIR HSI and (c) NIR HSI systems. (For interpretation of the references to colour in this figure legend, the reader is referred to the Web version of this article.)

3.4. Prediction models for moisture, antioxidant capacity and TPC

Table 2 shows the best performing models developed using the NIR-MEMS, Vis-NIR HSI and NIR HSI systems to predict moisture, DPPH, FRAP and TPC. These models were built using 120 randomly selected samples and validated using the remaining 41 samples.

The best prediction models developed using the NIR-MEMS performed very well for TPC (RPD 3.5–3.7), fairly for FRAP (RPD 2.5), poorly for moisture (RPD 2.3–2.5) and were not suitable for DPPH (RPD 1.8–2.1) prediction. The performance of the best prediction models

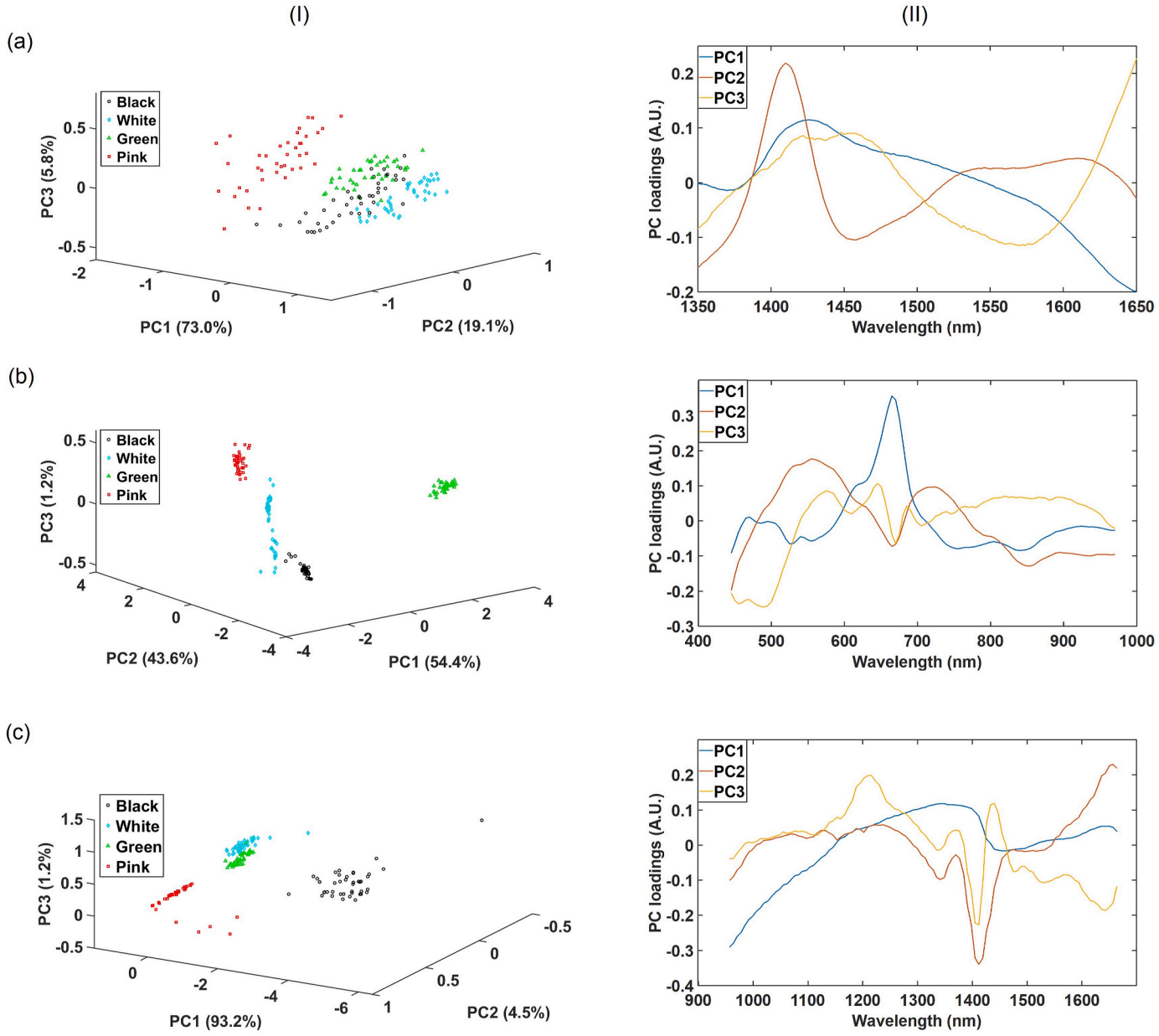

Fig. 2. Principal component analysis scores (I) and loadings (II) of the three first principal components (a) NIR-MEMS (b) Vis-NIR HSI (c) NIR-HSI SNV treated spectra of ground peppercorn samples.

developed using the Vis-NIR HSI and NIR HSI spectral ranges were similar for DPPH, FRAP and TPC yielding good (RPD 2.9–3.1), fair (RPD 2.8–2.9) and very good (RPD 3.8–4.1) predictions respectively. The best moisture content prediction model developed using the NIR HSI spectra yielded very good (RPD > 3.5) predictions, while the best model developed using the Vis-NIR HSI spectra yielded poor moisture content predictions (RPD 2.3–2.4). The very good performance of the models developed using the validation sets (Table 2) demonstrated the potential of NIR-MEMS and Vis-NIR/NIR HSI to predict the moisture content, antioxidant capacity and total phenolic content of peppercorns. Both technologies can be used for in-line control of multiple analytes in peppercorn processing.

Fig. 3 shows the selected bands for the best prediction models developed using the NIR HSI spectral range. The selected bands in the range 978, 1013–1160, 1083–1174, 1265–1286, 1342, 1405–1450,1461 - 1475 and 1538–1664 nm may be attributed to the second overtone O–H stretching, the second overtone of C–H stretching in $–CH_3$ groups, the combination of $–CH_2$, protein-water interaction, the first overtone of C–H stretching and C–H bending combination, first overtone O–H stretching of weak bonded water, first overtone O–H stretching of strong bonded water and first overtone of aromatic –CH respectively (Kumagai et al., 2003; Rodriguez-Saona et al., 2017; Šašić & Ozaki, 2000).

Due to the larger spectral range of the NIR HSI system, better prediction models were developed compared to the NIR-MEMS systems. However the prediction models developed using the NIR-MEMS spectra

Table 2
Performance of prediction models developed using MEMS NIR, Vis – NIR HSI and NIR HSI systems to predict moisture (g/100 g sample), DPPH (%), FRAP (mM TE/100 g sample) and TPC (mg GAE/100 g sample) of ground peppercorns.

	System	R/log(1/R)	Pre-treatment	N Bands	N LV	Cross Validation			Validation		
						RMSECV	RPDCV	R^2CV	RMSEP	RPDP	R^2P
Moisture	NIR-MEMS	R	MS + AsLS	19	5	1.0	2.3	0.80	1.1	2.5	0.84
	Vis-NIR HSI	log(1/R)	SNV+2Der	9	6	1.0	2.4	0.83	1.2	2.3	0.83
	NIR-HSI	**log(1/R)**	-	**25**	**7**	**0.7**	**3.5**	**0.92**	**0.8**	**3.7**	**0.93**
DPPH	NIR-MEMS	log(1/R)	MS+2Der	10	3	10.7	2.2	0.79	13.9	1.7	0.64
	Vis-NIR HSI	**R**	**MS + 1Der**	**9**	**3**	**7.6**	**3.1**	**0.90**	**7.9**	**3.0**	**0.89**
	NIR-HSI	**R**	**1Der**	**16**	**4**	**8.0**	**2.9**	**0.88**	**7.9**	**3.0**	**0.89**
FRAP	NIR-MEMS	R	SNV + LD	36	6	1452	2.5	0.84	1924	2.5	0.86
	Vis-NIR HSI	**R**	**2Der + SNV**	**6**	**4**	**1232**	**2.9**	**0.88**	**1651**	**2.8**	**0.88**
	NIR-HSI	**log(1/R)**	**LD + 2Der**	**31**	**5**	**1281**	**2.8**	**0.87**	**1670**	**2.9**	**0.90**
TPC	NIR-MEMS	log(1/R)	AsLs	30	6	340	3.5	0.92	395	3.7	0.93
	Vis-NIR HSI	**log(1/R)**	**LD + 1Der**	**5**	**3**	**317**	**3.8**	**0.93**	**357**	**4.1**	**0.94**
	NIR-HSI	**log(1/R)**	**LD**	**21**	**5**	**320**	**3.8**	**0.93**	**384**	**4.0**	**0.94**

The best models for each analyte are marked in bold. R: reflectance, N Bands: number of bands included in the model, N LV: number of latent variables used in the model, RMSE: root mean square error in cross validation, RPD: the ratio of standard deviation of the reference data of calibration set and the RMSECV, R^2: square of the coefficient of correlation, CV: crossvalidation, P: validation set, MS: median centred, AsLs: asymmetric least squares, SNV: standard normal variate, 2Der: second derivative, 1Der: first derivative, LD: linear detrending.

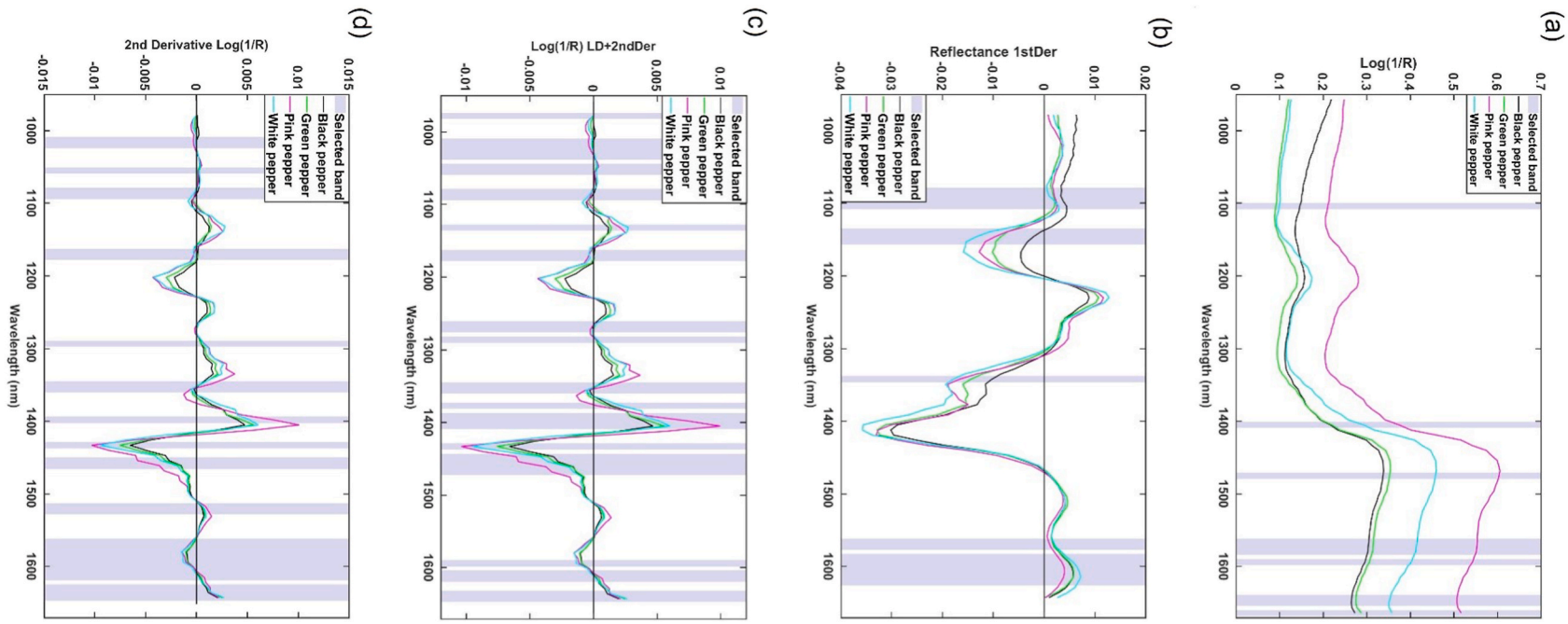

Fig. 3. Mean ground peppercorn NIR-HSI pretreated spectra and selected bands for (a) moisture, (b) DPPH, (c) FRAP and (d) TPC prediction.

performed very well for TPC and fairly for FRAP. Sensor fusion of multiple complementary NIR MEMS systems based on FPIs could be employed to extend the total spectral range measured for model development and improve prediction performance.

4. Conclusions

This study demonstrated the potential of an NIR MEMS spectrophotometer and Vis-NIR/NIR hyperspectral imaging systems to predict moisture content, antioxidant capacity and total phenolic content properties of ground peppercorns. The potential of the NIR-MEMS spectrophotometer for food applications was demonstrated through prediction models developed for FRAP (RPD > 2.4) and total phenolic content (RPD > 3.6) of ground peppercorns. Both HSI systems investigated were demonstrated to be suitable for use as rapid process analytical tools for evaluation of antioxidant capacity (DPPH RPD > 3.0, FRAP RPD > 2.9) and TPC (RPD > 3.8) of ground peppercorns. The NIR HSI system has the additional benefit of very good moisture content prediction. Sensor fusion of multiple complementary NIR MEMS systems based on FPIs could be employed to extend the spectral range for model development and improve prediction performance. Band selection and spectral pre-treatments were key for robust prediction model development. The three spectroscopy systems investigated may be employed as in-line PAT tools to provide improved control and understanding in peppercorn processing.

Funding

This research did not receive any specific grant from funding agencies in the public, commercial, or not-for-profit sectors.

Declaration of competing interest

The authors declare no conflict of interest.

CRediT authorship contribution statement

Carlos A. Esquerre: Conceptualization, Methodology, Software, Formal analysis, Writing - original draft, Writing - review & editing. **Eva M. Achata:** Investigation, Data curation. **Marco García-Vaquero:** Conceptualization, Methodology, Investigation. **Zhihang Zhang:** Investigation, Data curation. **Brijesh K. Tiwari:** Conceptualization, Methodology, Supervision. **Colm P. O'Donnell:** Conceptualization, Methodology, Writing - review & editing, Supervision.

References

Achata, E. M., Esquerre, C., O'Donnell, C. P., & Gowen, A. A. (2015). A study on the application of near infrared hyperspectral chemical imaging for monitoring moisture content and water activity in low moisture systems. *Molecules, 20*(2), 2611–2621. https://doi.org/10.3390/molecules20022611.

Achata, E. M., Inguglia, E. S., Esquerre, C., Tiwari, B. K., & O'Donnell, C. P. (2019). Evaluation of Vis-NIR hyperspectral imaging as a process analytical tool to classify brined pork samples and predict brining salt concentration. *Journal of Food Engineering, 246*, 134–140. https://doi.org/10.1016/j.jfoodeng.2018.10.022.

Benzie, I. F. F., & Strain, J. J. (1996). The ferric reducing ability of plasma (FRAP) as a measure of "antioxidant power": The FRAP assay. *Analytical Biochemistry, 239*(1), 70–76. https://doi.org/10.1006/abio.1996.0292.

Charoux, C. M. G., Free, L., Hinds, L. M., Vijayaraghavan, R. K., Daniels, S., O'Donnell, C. P., et al. (2020). Effect of non-thermal plasma technology on microbial inactivation and total phenolic content of a model liquid food system and black pepper grains. *Lebensmittel-Wissenschaft & Technologie, 118*, Article 108716. https://doi.org/10.1016/j.lwt.2019.108716.

Esquerre, C., Gowen, A. A., Burger, J., Downey, G., & O'Donnell, C. P. (2012). Suppressing sample morphology effects in near infrared spectral imaging using chemometric data pre-treatments. *Chemometrics and Intelligent Laboratory Systems*. https://doi.org/10.1016/j.chemolab.2012.02.006 117(0), 129-137.

Esquerre, C., Gowen, A. A., O'Gorman, A., Downey, G., & O'Donnell, C. P. (2017). Evaluation of ensemble Monte Carlo variable selection for identification of metabolite markers on NMR data. *Analytica Chimica Acta, 964*, 45–54. https://doi.org/10.1016/j.aca.2017.01.027.

Friedman, M., Levin, C. E., Lee, S.-U., Lee, J.-S., Ohnisi-Kameyama, M., & Kozukue, N. (2008). Analysis by HPLC and LC/MS of pungent piperamides in commercial black, white, green, and red whole and ground peppercorns. *Journal of Agricultural and Food Chemistry, 56*(9), 3028–3036. https://doi.org/10.1021/jf703711z.

Ganesan, P., Kumar, C. S., & Bhaskar, N. (2008). Antioxidant properties of methanol extract and its solvent fractions obtained from selected Indian red seaweeds. *Bioresource Technology, 99*(8), 2717–2723. https://doi.org/10.1016/j.biortech.2007.07.005.

Garcia-Vaquero, M., O'Doherty, J. V., Tiwari, B. K., Sweeney, T., & Rajauria, G. (2019). Enhancing the extraction of polysaccharides and antioxidants from macroalgae using sequential hydrothermal-assisted extraction followed by ultrasound and thermal technologies. *Marine Drugs, 17*(8), 457. https://doi.org/10.3390/md17080457.

Gomes, R. B.d. A., de Souza, E. S., Gerhardt Barraqui, N. S., Tosta, C. L., Nunes, A. P. F., Schuenck, R. P., … Kuster, R. M. (2020). Residues from the Brazilian pepper tree (Schinus terebinthifolia Raddi) processing industry: Chemical profile and antimicrobial activity of extracts against hospital bacteria. *Industrial Crops and Products, 143*, Article 111430. https://doi.org/10.1016/j.indcrop.2019.05.079.

Gowen, A. A., Downey, G., Esquerre, C., & O'Donnell, C. P. (2011). Preventing over-fitting in PLS calibration models of near-infrared (NIR) spectroscopy data using regression coefficients. *Journal of Chemometrics, 25*(7), 375–381. https://doi.org/10.1002/cem.1349.

Gowen, A. A., O'Donnell, C. P., Cullen, P. J., Downey, G., & Frias, J. M. (2007). Hyperspectral imaging - an emerging process analytical tool for food quality and safety control. *Trends in Food Science & Technology, 18*(12), 590–598. https://doi.org/10.1016/j.tifs.2007.06.001.

Hernández-Hierro, J. M., Esquerre, C., Valverde, J., Villacreces, S., Reilly, K., Gaffney, M., … Downey, G. (2014). Preliminary study on the use of near infrared hyperspectral imaging for quantitation and localisation of total glucosinolates in freeze-dried broccoli. *Journal of Food Engineering, 126*, 107–112. https://doi.org/10.1016/j.jfoodeng.2013.11.005.

Kumagai, M., Suyama, H., Sato, T., Amano, T., Kikuchi, R., & Ogawa, N. (2003). Chemical meaning of near infrared spectra from a portable near infrared spectrometer for various plastic wastes. *International Journal of the Society of Materials Engineering for Resources, 11*(1), 5–9. https://doi.org/10.5188/ijsmer.11.5.

Lapcharoensuk, R., Chalachai, S., Sinjaru, S., Singsriand, P., Hongwiangjan, J., & Yaemphochai, N. (2019). Quantitative detection of pepper powder adulterated with rice powder using Fourier-transform near infrared spectroscopy. *Paper presented at the IOP conference series: Earth and environmental science*.

Meghwal, M., & Goswami, T. K. (2013). Piper nigrum and piperine: An update. *Phytotherapy Research, 27*(8), 1121–1130. https://doi.org/10.1002/ptr.4972.

Mendelson, Y. (2012). Chapter 10 - biomedical Sensors. In J. D. Enderle, & J. D. Bronzino (Eds.). *Introduction to biomedical engineering* (pp. 609–666). (3rd ed). Boston: Academic Press.

Misra, N. N., Patil, S., Moiseev, T., Bourke, P., Mosnier, J. P., Keener, K. M., et al. (2014). In-package atmospheric pressure cold plasma treatment of strawberries. *Journal of Food Engineering, 125*, 131–138. https://doi.org/10.1016/j.jfoodeng.2013.10.023.

Montenegro, J., Ruan, R., Ma, H., & Chen, P. (2002). Inactivation of E. coli O157:H7 using a pulsed nonthermal plasma system. *Journal of Food Science, 67*(2), 646–648. https://doi.org/10.1111/j.1365-2621.2002.tb10653.x.

Mujica, L. E., Rodellar, J., Fernández, A., & Güemes, A. (2010). Q-statistic and T2-statistic PCA-based measures for damage assessment in structures. *Structural Health Monitoring, 10*(5), 539–553. https://doi.org/10.1177/1475921710388972.

Nicklisch, S. C. T., & Waite, J. H. (2014). Optimized DPPH assay in a detergent-based buffer system for measuring antioxidant activity of proteins. *MethodsX, 1*, 233–238. https://doi.org/10.1016/j.mex.2014.10.004.

Nikolić, M., Stojković, D., Glamočlija, J., Ćirić, A., Marković, T., Smiljković, M., et al. (2015). Could essential oils of green and black pepper be used as food preservatives? *Journal of Food Science and Technology, 52*(10), 6565–6573. https://doi.org/10.1007/s13197-015-1792-5.

O'Donnell, C. P., Fagan, C., & Cullen, P. J. (2014). *Process analytical technology for the food industry*.

Orrillo, I., Cruz-Tirado, J. P., Cardenas, A., Oruna, M., Carnero, A., Barbin, D. F., et al. (2019). Hyperspectral imaging as a powerful tool for identification of papaya seeds in black pepper. *Food Control, 101*, 45–52. https://doi.org/10.1016/j.foodcont.2019.02.036.

Parashar, A., Shah, A., Packirisamy, M., & Sivakumar, N. (2007). Three cavity tunable MEMS Fabry perot interferometer. *Sensors, 7*(12), 3071–3083. https://doi.org/10.3390/s7123071.

Plessi, M., Bertelli, D., & Miglietta, F. (2002). Effect of microwaves on volatile compounds in white and black pepper. *Lebensmittel-Wissenschaft und -Technologie- Food Science and Technology, 35*(3), 260–264. https://doi.org/10.1006/fstl.2001.0853.

Pu, Y.-Y., O'Donnell, C., Tobin, J. T., & O'Shea, N. (2020). Review of near-infrared spectroscopy as a process analytical technology for real-time product monitoring in dairy processing. *International Dairy Journal, 103*, Article 104623. https://doi.org/10.1016/j.idairyj.2019.104623.

Rodriguez-Saona, L. E., & Aykas, D. P. (2019). New approaches for rapid tomato quality control. In S. Porretta (Ed.). *Tomato chemistry, industrial processing and product development*.

Rodriguez-Saona, L. E., Ayvaz, H., & Wehling, R. L. (2017). Infrared and Raman spectroscopy. In S. Nielsen (Ed.). *Food analysis* (pp. 107–127). Springer.

Šašić, S., & Ozaki, Y. (2000). Band Assignment of near-infrared spectra of milk by use of partial least-squares regression. *Applied Spectroscopy, 54*(9), 1327–1338.

Schiffmann, R. F. (2014). Microwave and dielectric drying. In A. S. Mujumdar (Ed.). *Handbook of industrial drying*. CRC Press.

Schulz, H., Baranska, M., Quilitzsch, R., Schütze, W., & Lösing, G. (2005). Characterization of peppercorn, pepper oil, and pepper oleoresin by vibrational

spectroscopy methods. *Journal of Agricultural and Food Chemistry, 53*(9), 3358–3363. https://doi.org/10.1021/jf048137m.

Segtnan, V. H., Sasic, S., Isaksson, T., & Ozaki, Y. (2001). Studies on the structure of water using two-dimensional near-infrared correlation spectroscopy and principal component analysis. *Analytical Chemistry, 73*(13), 3153–3161. https://doi.org/10.1021/ac010102n.

Seifert, B., & Zude-Sasse, M. (2016). High hydrostatic pressure effects on spectral-optical variables of the chlorophyll pool in climacteric fruit. *Lebensmittel-Wissenschaft & Technologie, 73*, 303–310. https://doi.org/10.1016/j.lwt.2016.06.011.

Shityakov, S., Bigdelian, E., Hussein, A. A., Hussain, M. B., Tripathi, Y. C., Khan, M. U., et al. (2019). Phytochemical and pharmacological attributes of piperine: A bioactive ingredient of black pepper. *European Journal of Medicinal Chemistry, 176*, 149–161. https://doi.org/10.1016/j.ejmech.2019.04.002.

Wang, Y.-C., Shyu, L.-H., & Chang, C.-P. (2010). The comparison of environmental effects on Michelson and fabry-perot interferometers utilized for the displacement measurement. *Sensors, 10*(4), 2577–2586. https://doi.org/10.3390/s100402577.

Wilde, A. S., Haughey, S. A., Galvin-King, P., & Elliott, C. T. (2019). The feasibility of applying NIR and FT-IR fingerprinting to detect adulteration in black pepper. *Food Control, 100*, 1–7. https://doi.org/10.1016/j.foodcont.2018.12.039.

Williams, P. (2014). The RPD statistic: A tutorial note. *NIR News, 25*(1), 22–26. https://doi.org/10.1255/nirn.1419.

Yan, H., & Siesler, H. W. (2018). Identification performance of different types of handheld near-infrared (NIR) spectrometers for the recycling of polymer commodities. *Applied Spectroscopy, 72*(9), 1362–1370. https://doi.org/10.1177/0003702818777260.

Zimmerleiter, R., Kager, J., Nikzad-Langerodi, R., Berezhinskiy, V., Westad, F., Herwig, C., et al. (2019). Probeless non-invasive near-infrared spectroscopic bioprocess monitoring using microspectrometer technology. *Analytical and Bioanalytical Chemistry*. https://doi.org/10.1007/s00216-019-02227-w.